2024-1380 IJOI
https://www.ijoi-online.org/

International Journal of Organizational Innovation

LANDSLIDE PROBLEMS CAUSED BY EXCAVATION OF SHEAR BAND TUNNELS INTO GRABENS

Tse-Shan Hsu
President, Institute of Mitigation for Earthquake Shear Banding Disasters
Professor, Feng-Chia University, Taiwan, R.O.C., tshsu@fcu.edu.tw

Yan-Ming Wang
Director, Institute of Mitigation for Earthquake Shear Banding Disasters, Taiwan, R.O.C.

Yu-Chien Wu
Ph.D. Student, Ph.D. Program for Infrastructure Planning and Engineering,
Feng-Chia University, Taiwan, R.O.C.

Zong-Lin Wu
Assistant Professor, National Chin-Yi University of Technology, Taiwan, R.O.C.

Si-Min Hsu
Member, Institute of Mitigation for Earthquake Shear Banding Disasters, Taiwan, R.O.C.

Abstract

The Zhongliao Tunnel of Formosa Highway No. 3 was completed in 2000. The tunnel passes through shear bands, but the engineers overlooked the tilting effects of shear banding during design, resulting in ongoing uplift issues at the north portal of the tunnel. Following this, the consulting firm responsible for the tunnel design proposed mitigating the uplift by excavating the shear band section at the north portal of the tunnel into a graben. A similar section of the national highway was destroyed by a landslide induced by shear band graben slope sliding near Keelung in 2010. If the north portal of the Zhongliao Tunnel is excavated into a shear band graben, it is likely to replicate this landslide disaster, which shocked the international community. For this reason, the authors of this paper

conducted stability analysis on the slope of the shear band graben excavated at the north portal of the Zhongliao Tunnel and drew the following three conclusions. (1) A shear zone tunnel presents only local instability problems and does not induce overall tunnel instability. (2) After the shear zone tunnel is excavated into a cutting, the slope of the shear zone cutting is prone to sliding failure. (3) The primary factors that induce the instability of the graben slope in a shear band is the infiltration groundwater, which fills the pore space in the shear band, and the softening of shear resistance due to shear banding. Based on these conclusions, the authors recommend that future stability analyses of retaining wall slopes must account for shear banding effects and thus avoid the excavation of faults or shear zones in shear band graben slopes. These measures can help mitigate sliding damage of the graben slope and ensure the safety of the public.

Keywords: fault, shear band, highway, tunnel, graben.

Introduction

Because of its unique geographical location, Taiwan experiences frequent tectonic earthquakes. When the Eurasian Plate is continuously compressed laterally and the strain enters the plastic range, the plate undergoes strain softening and generates shear bands. Ground vibration is caused by the shear banding, which is the primary effect of tectonic earthquakes, while ground vibration is a secondary effect.

In the past, seismic design specifications for various structures only focused on fortifying against ground vibration, completely overlooking the influence of shear banding. As a result, the 3.1K ground anchor retaining wall slope on Formosa Highway No. 3 (Hsu et al., 2018)), designed with a lifespan exceeding 50 years, was damaged by sliding only 6 years after completion because of excessive accumulation of shear banding (see Figure 1).

Figure 1. Sliding failure of the anchor retaining wall slope on Formosa Highway No. 3 at 3.1K (Taiwan Geotechnical Society, 2011).

Figure 2 shows the cliffs at 3.1K on Formosa Highway No. 3, which are displaced landforms resulting from shear banding. It is evident that the shear band slope of Formosa Highway No. 3 shown in Figure 1 was excavated into a graben, and one side of the graben's shear band slope began to slide downwards after completion, leading to a major landslide disaster 6 years later.

(a) Before drawing the shear textures (Google Earth, 2019).

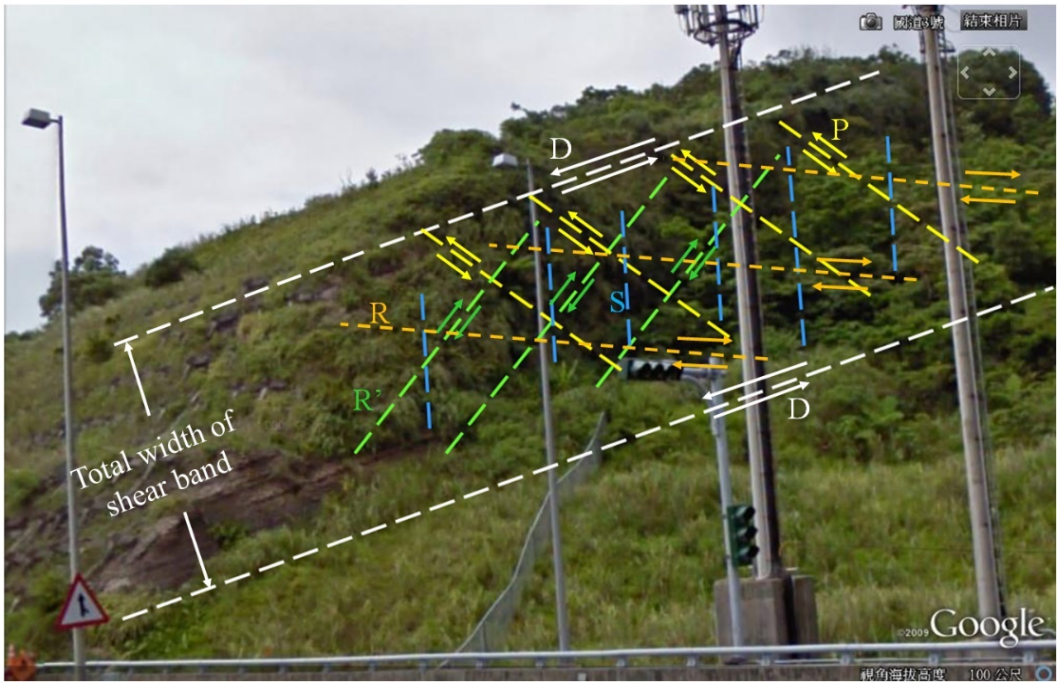

(b) After drawing the shear textures (Background image from Google Earth, 2019).

Figure 2. Shear textures at the 3.1K slope of Formosa Highway No. 3.

Figure 3 shows the north tunnel entrance of the Zhongliao Tunnel on a different section of Formosa Highway No. 3. According to on-site surveys, the Qishan Fault is encountered approximately 50 m after entering the north tunnel entrance, so that the tunnel is affected by Qishan faulting. Since completion of the tunnel and opening it to traffic in February 2000, the north side of the Qishan Fault has risen by 115 cm. The government therefore aims to address this problem by implementing the project.

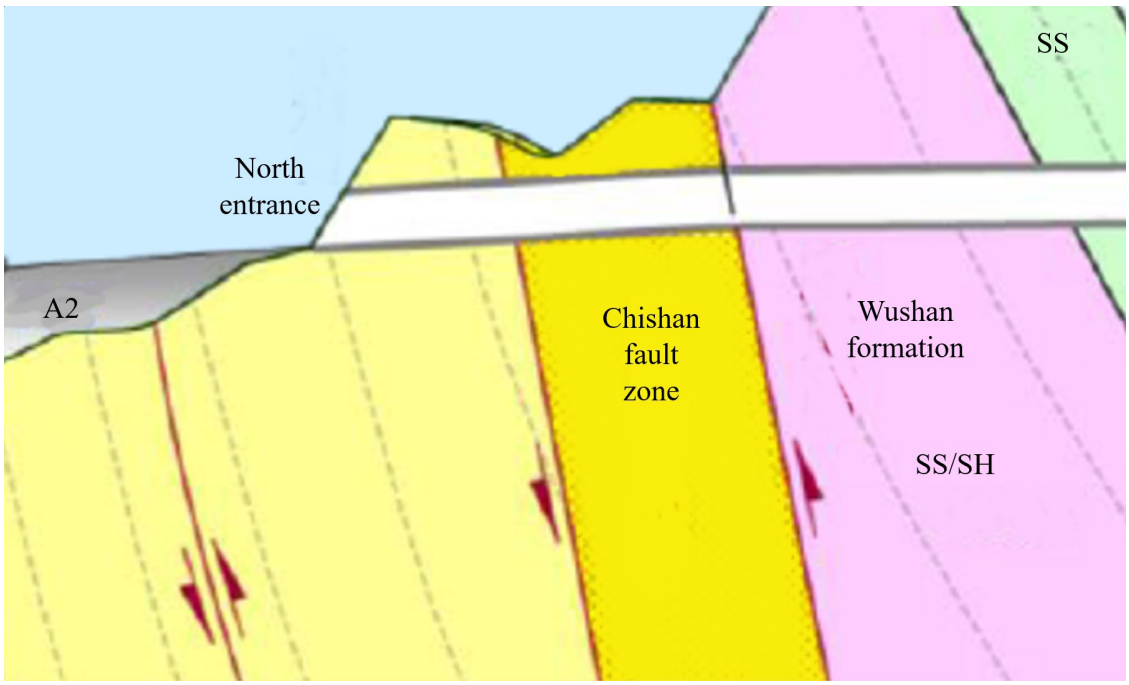

Figure 3. North entrance of Zhongliao Tunnel at Formosa No. 3 Highway 378K is excavated into a shear zone graben (Taiwan Highway Bureau, Ministry of Transportation and Communications, 2016).

However, the improvement project proposed by the government involves excavating the north entrance of the Zhongliao Tunnel into a shear band graben. Therefore, the potential sliding failure mechanism of the graben slope is the same as the sliding failure mechanism of the 3.1K graben slope of Formosa Highway No. 3.

Because the engineering consulting company commissioned by the Highway Bureau of the Ministry of Transportation did not consider the concept of shear banding, the influence of shear banding was not included in the design; therefore, because the north portal of Zhongliao Tunnel was excavated into the graben, sliding failure of the shear band slope cannot be avoided.

The authors of this paper will account for the actual sliding failure mechanism of shear banding tilting slopes in slope stability analysis. They will explore how the graben slope, considered stable in the original design, will slide and fail under shear banding, for the purpose of reminding road users to exercise increased vigilance when passing through tunnels in shear band grabens.

Shear Band Displaced Landform Features

Figure 4 shows the mountain traversed by the Zhongliao Tunnel. Shear band displaced landform features include winding and undulating ridge lines, exposed shear banded rocks, dense omega-shaped bends, and a mountain lake on the top of the mountain.

Note: The yellow needle points to the mountain lake.

(a) Overall view (Google Earth, 2019).

（b）Mountain lake (Google Earth, 2019).

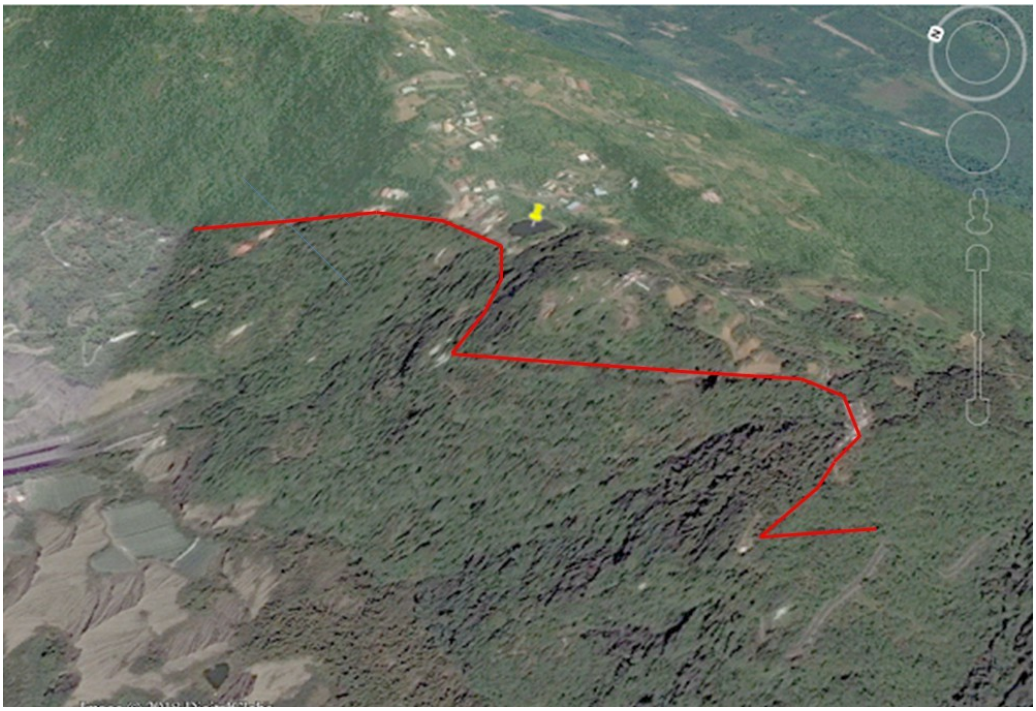

（c）Ω-shaped bends typical of mountainous regions (Background image from Google Earth, 2019).

Figure 4. Shear band displaced landform features near the Zhongliao Tunnel.

Influence of a Mountain Lake

In the presence of a mountain lake, produced by the tilting effect of the shear zone as shown in Figure 4, lake water fills the pore spaces of brittle fractured shear bands with the result that landslides on the shear band slope below the lake are more likely to occur. Before excavation into the graben at the north entrance of the Zhongliao Tunnel, the intact tunnel structure restrained faulting, causing only localized fractures from the Qishan Fault without inducing large-scale collapse damage to the tunnel. However, when the north entrance of the tunnel is excavated into a graben, the Qishan Fault is exposed on both sides of the graben slopes. Therefore, the dislocation of the fault and the water derived from the mountain lake are detrimental to the stability of the graben slope. For the Zhongliao Tunnel, the possible range of influence of the mountain lake water when the north entrance tunnel is excavated into the graben is shown in Figure 5.

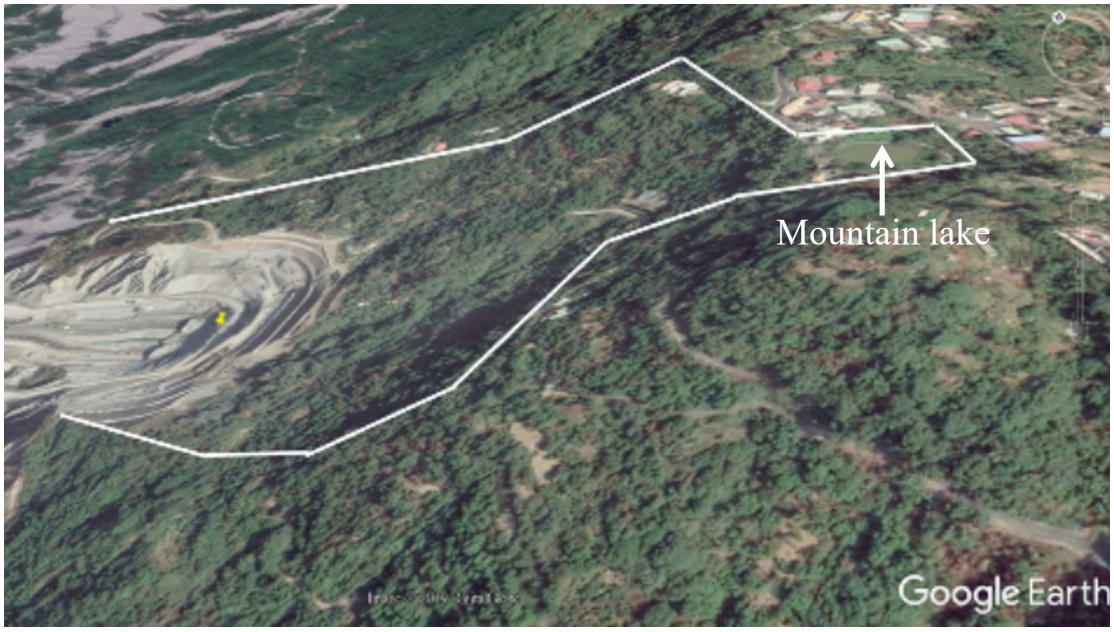

Figure 5. The area of influence of water from the mountain lake above the Zhongliao Tunnel (Background image from Google Earth, 2019).

Shear Textures in the Mountainous Area of Zhongliao Tunnel

When the north entrance of the Zhongliao Tunnel was excavated into the graben, as shown in Figure 6, the principal displacement shear D, thrust shear P, Riedel shear R, conjugate Riedel shear R', and compression textures S contained within the total width of the shear band developed, and these affect the stability of the graben slope.

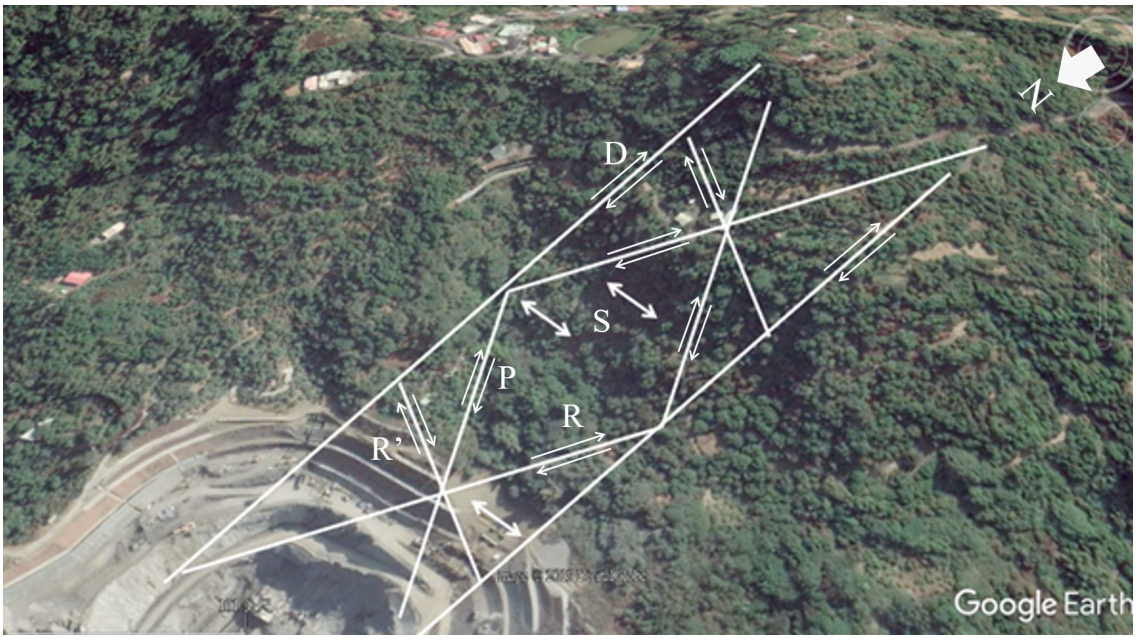

Figure 6. Shear band and shear textures observed after the graben was excavated at the north entrance of the tunnel (Background image from Google Earth, 2019).

Under the influence of shear banding and shear texturing, as shown in Figure 7, the slope above the tunnel remained unstable during the excavation of the north entrance of the Zhongliao Tunnel into the graben.

Figure 7. Instability of the slope during the excavation process of the north entrance of the Zhongliao Tunnel into the graben.

Slope Stability Analysis in the Mountainous Area of Zhongliao Tunnel

As shown in Figure 6, shear textures such as the principal displacement shear D, thrust shear P, Riedel shear R, conjugate Riedel shear R', and compression textures S are observed with different strikes within the total shear band width, and shear banding and shear texturing cause slope instability problems with double sliding surfaces. Therefore, the slope stability analysis method of double sliding surfaces will be used in this study to conduct slope stability analysis.

Slope Stability Analysis Method with Double Sliding Surfaces

For the slope with double sliding surfaces, Figure 8 shows the various forces and sliding resistances acting on the double sliding surfaces and the upper and lower sliding blocks.

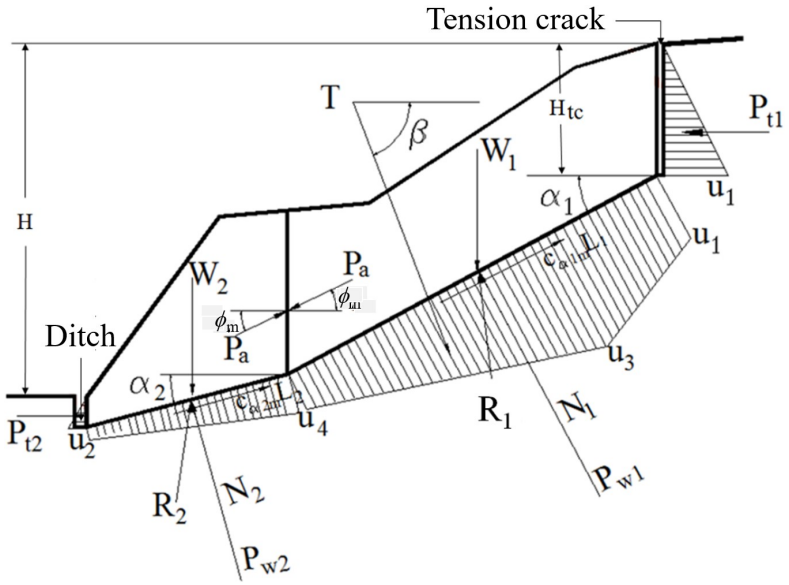

Note: T represents anchor tension.

Figure 8. Forces and sliding resistances acting on double sliding surfaces and upper and lower sliding blocks.

In Figure 8, H denotes the total slope height, H_{tc} denotes the depth of the tension crack, W_1 denotes the weight of the upper sliding block, P_a denotes the active earth pressure, ϕ_m denotes the angle between P_a and the horizontal, L_1 denotes the length of the upper sliding surface, α_1 denotes the angle between the upper sliding surface and the horizontal plane, $c_{\alpha 1}$ denotes the adhesion between the upper sliding block and the adjacent stable block, $\delta_{\alpha 1}$ denotes the friction angle between the upper sliding block and the adjacent stable block, N_1 denotes the reaction force of W_1 in the vertical direction of the upper sliding surface, P_{w1} denotes the resultant force of the water pressure acting on the upper sliding surface, P_{t1} denotes the water pressure at the bottom of the tension crack after the depth of the tension crack in the upper sliding block is filled with water, and P_{t1} denotes the resultant force of water pressure generated after the aforementioned tension crack is filled with water.

The action and resistance forces on the lower and upper sliding blocks are depicted in the force polygons shown in Figures 9(a) and 9(b), respectively.

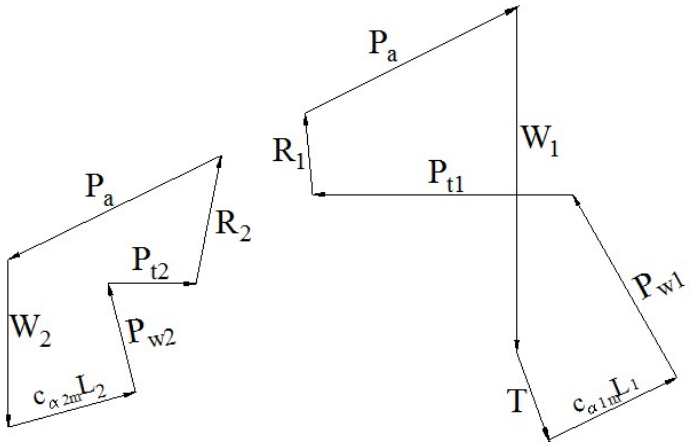

Figure 9. Force polygons for the lower and the upper sliding blocks.

Under force equilibrium, the force polygons for all the forces of the upper and lower sliding blocks must be closed. By applying the force polygon of the closing force of the upper sliding block, the following equation can be derived:

$$P_a = A^* / [\cos\phi_m + \sin\phi_m \tan(\alpha_1 - \delta_{1m})] \tag{1}$$

In Equation 1,

$$\begin{aligned} A^* = {} & \left(W_1 + T\sin\beta - P_{w1}\cos\alpha_1 - c_{\alpha 1m}L_1\sin\alpha_1\right)\tan(\alpha_1 - \delta_{1m}) \\ & + P_{t1} + P_{w1}\sin\alpha_1 - c_{\alpha 1m}L_1\cos\alpha_1 - T\cos\beta \end{aligned} \tag{2}$$

For the lower sliding block, the closed force cable polygon can be obtained:

$$P_a = B^* / [\cos\phi_m + \sin\phi_m \tan(\alpha_2 - \delta_{2m})] \tag{3}$$

In Equation 3,

$$\begin{aligned} B^* = {} & P_{t2} + c_{\alpha 2m}L_2\cos\alpha_2 - P_{w2}\cos_{\alpha 2} \\ & - \left(W_2 - P_{w2}\cos\alpha_2 - c_{\alpha 2m}L_2\sin\alpha_2\right)\cdot\tan(\alpha_2 - \delta_{2m}) \end{aligned} \tag{4}$$

The overall slope safety factor *FS* against sliding resistance applies to both the upper and lower sliding blocks. The active earth pressure P_a obtained from the closed force polygon of the upper and lower sliding blocks must be consistent, meaning that P_a obtained using Equation 1 and Equation 3 must be identical. Therefore, the safety factor *FS* against overall slope sliding resistance is determined through a trial-

and-error method and the following calculation procedure:

Step 1: The program is initiated with a sufficiently small *FS* value (for example, *FS* = 0.1) and a suitably small error tolerance (for example 0.01). The program is initiated with a sufficiently small *FS* value (for example, *FS* = 0.1) and a suitably small error tolerance (for example 0.01).

Step 2: $\phi_m = \phi / FS$,
$\delta_{1m} = \delta_1 / FS$, $\delta_{2m} = \delta_2 / FS$,
$c_{a1m} = c_{a1} / FS$,
$c_{a2m} = c_{a2} / FS$ are calculated.

Step 3: The active earth pressure of the upper sliding block is calculated as P_{a1} through equation 1. The active earth pressure of the lower sliding block is calculated as P_{a2} through equation 2. Then, the absolute value of the difference between P_{a1} and P_{a2} (i.e., $\Delta = |P_{a1} - P_{a2}|$) is calculated.

Step 4: When $\Delta \le \varepsilon$, after the safety factor *FS* is obtained, the program is stopped. When $\Delta > \varepsilon$, the safety factor is set to $FS = FS + 0.001$, and Step 2 is reiterated so that the program execution is continued.

Slope Stability Analysis After Graben Excavation at the North Entrance of Zhongliao Tunnel

Figure 10 shows the shear banding tilting slope after graben excavation at the north entrance of Zhongliao Tunnel. During the slope stability analysis process, the slope stability of block ABGF sliding along the potential sliding surfaces AB and BG was first analyzed. Second, the slope stability analysis of block BCKHG sliding along the potential sliding planes BC and CK was performed. Finally, the slope stability analysis of block CDENK sliding along the potential sliding surfaces CD and DE was carried out.

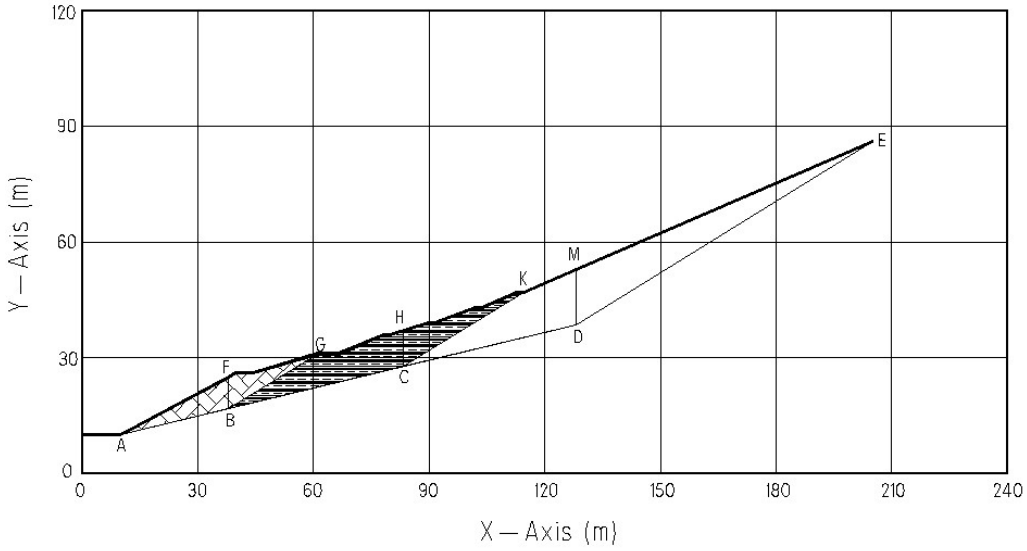

Figure 10. Profile of the shear banding tilting slope after graben excavation at the north entrance of the Zhongliao Tunnel.

During the slope stability analysis of the above three potential sliding blocks, the following three conditions must be fulfilled, respectively:

1) the impact of shear zone dislocation and groundwater are considered;

2) the impact of shear zone dislocation is overlooked, but the impact of groundwater is considered;

3) the impact of shear zone dislocation is considered, but the impact of groundwater is overlooked.

Figures 11(a) to 11(c) show cross-sections of the three double sliding blocks ABGF, BCKHG, and CDEMK after graben excavation at the north entrance of Zhongliao Tunnel. Given that the sliding surface is caused by groups of interlaced shear bands and shear textures, the angles between the upper sliding surface and the horizontal plane of the three selected sliding blocks are all 31.65°, and the angle between the lower sliding surface and the horizontal plane is 13.59°; the internal friction angle of the vertical interface selected to distinguish the upper sliding block and the lower sliding block is 30°, and the adhesion force of the upper sliding surface and the lower sliding surface is $3\ \mathrm{kN/m^2}$; the friction angles of the upper sliding surface and the lower sliding surface are both 30°, and the unit weight of the water is $9.807\ \mathrm{kN/m^3}$.

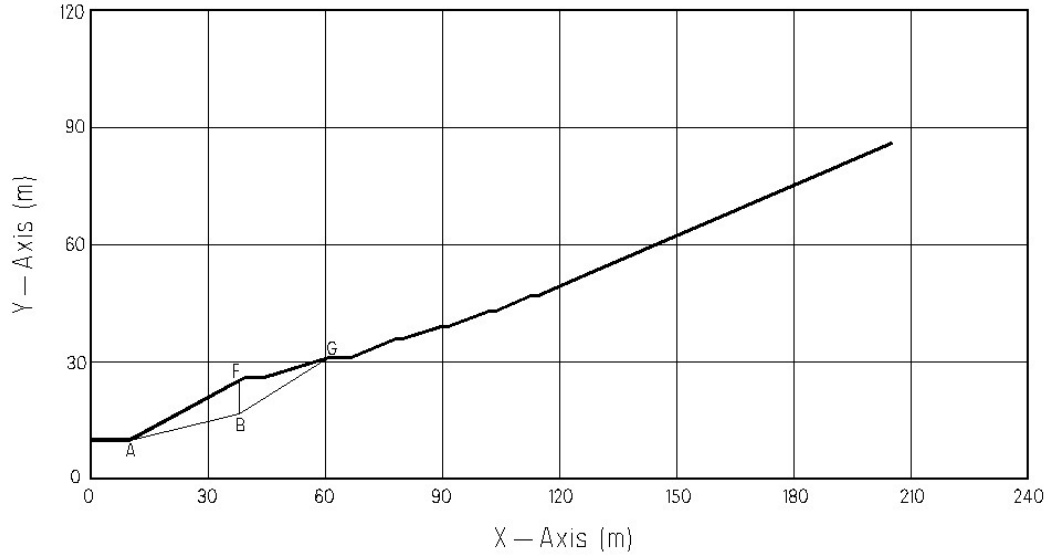

(a) block ABGF.

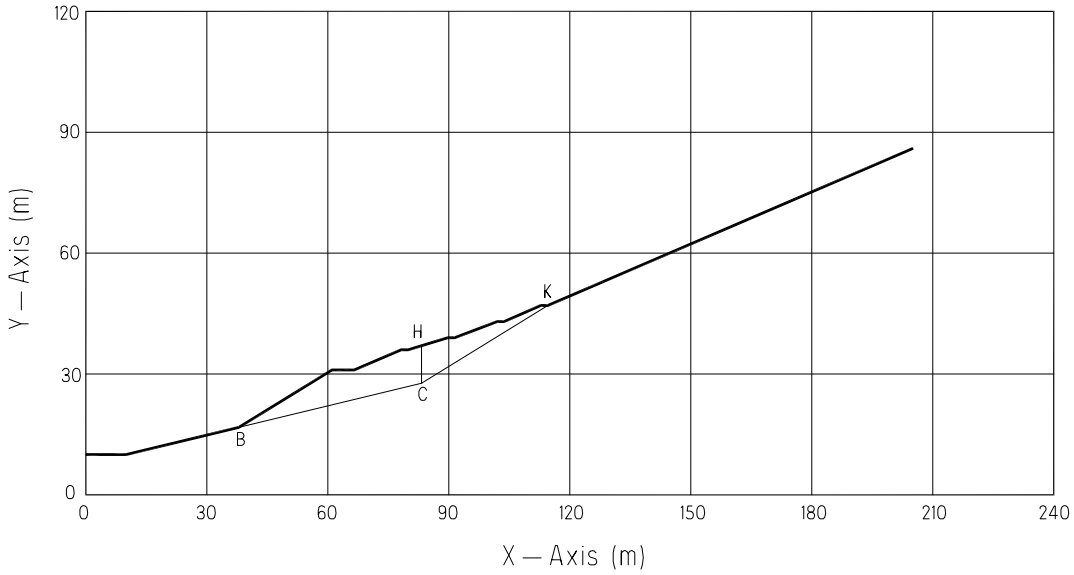

(b) block BCKHG.

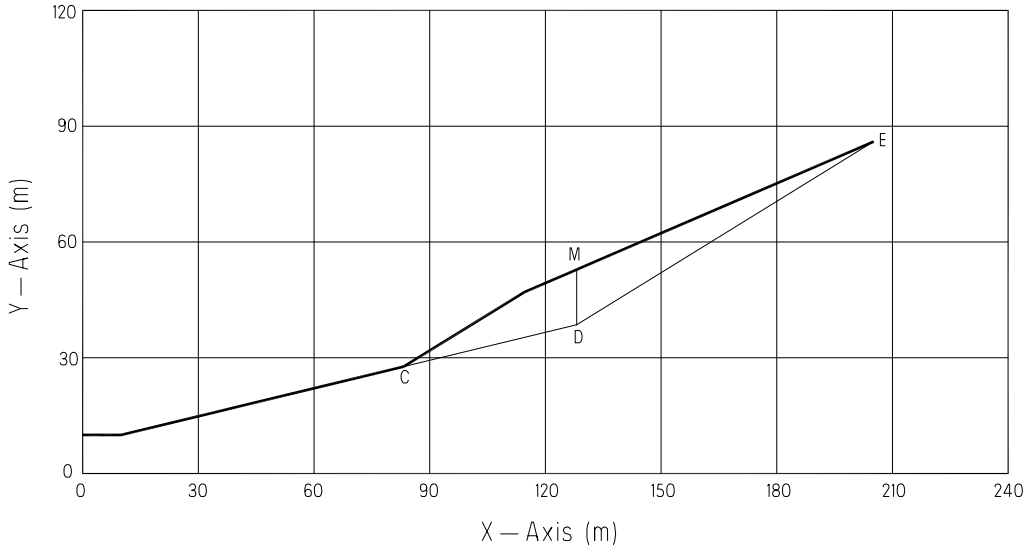

(c) block CDEMK.

Figure 11. Profiles of three double sliding surfaces after excavation of the graben at the north entrance of Zhongliao Tunnel.

Comparison and Discussion

For the graben slope adjacent to the north entrance of the Zhongliao Tunnel, the data in Table 1 indicate that when the potential sliding block is ABGF, this block has the potential for sliding failure only when the analysis considers the influence of groundwater or shear zone dislocation, i.e., when the safety factor against slope sliding failure *FS* is less than 1.0.

Table 1. Slope stability analysis results for the graben slope adjacent to the north entrance of the Zhongliao Tunnel.

Sliding block	Analysis conditions	Factor of safety, FS
ABGF	Neither shear banding nor groundwater is considered .	1.593
	Groundwater is considered, but shear banding is not.	0.869
	Shear banding is considered, but groundwater is not.	0.964
BCKHG	Neither shear banding nor groundwater is considered consid-ered.	1.742
	Groundwater is considered, but shear banding is not.	0.907
	Shear banding is considered, but groundwater is not.	1.069
CDEMK	Neither shear banding nor groundwater is considered consid-ered	1.347
	Groundwater is considered, but shear banding is not.	0.131
	Shear banding is considered, but groundwater is not.	0.837

For the same graben slope, Table 1 indicates that when block ABGF slides and fails, and the potential sliding block is BCKHG, *FS* obtained through the slope stability analysis is less than 1.0 under the influence of groundwater, indicating that block BCKHG has the potential for sliding failure. Under the influence of shear banding, *FS* is slightly greater than 1.0, indicating that block BCKHG is approaching sliding failure.

When both blocks ABGF and BCKHG slide and fail, and the potential sliding block is CDEMK, *FS* obtained from the slope stability analysis is less than 1.0 under the influence of

groundwater or shear banding, indicating that block CDEMK, and thus all blocks, may experience sliding failure For this case (lower third of Table 1), *FS* is considerably less than 1.0, indicating that the CDEMK block has a very high sliding failure potential.

When the planned excavation at the north entrance of Zhongliao Tunnel into the graben commences, the sliding blocks will have a high potential for failure. The reason for this is that the shear band has a high permeability coefficient and water from the mountain lake is likely to infiltrate and fill the void space in the shear zone, thus reducing *FS* obtained from the slope stability analysis to values far less than 1.0.

For the north entrance of Zhongliao Tunnel on Formosa No. 3 Highway, when the graben slope block ABGF adjacent to the north entrance slides and fails, block BCKHG above it is also at risk of sliding and failing; failure of both blocks ABGF and BCKHG increases the risk of sliding and failing for block CDEMK above them.

According to the aforementioned results, in the design of Formosa No. 3 Highway, Zhongliao Tunnel was misguidedly planned to be under the mountain lake. This can be attributed to the lack of professional knowledge regarding shear bands among the engineers. As a result, the Zhongliao Tunnel was excavated into a graben and the Qishan Fault, causing the graben slope to become unstable under the influence of groundwater and shear banding.

Conclusions and Suggestions

In 2010, the shear banding graben slope of Formosa No. 3 Highway at 3.1K experienced sliding failure 6 years after completion. This occurred without wind, rain, or earthquake. In 2018, a similar shear banding graben slope was excavated at the north entrance of the 378K Zhongliao Tunnel on Formosa No. 3 Highway. Because of the presence of a mountain lake above the tunnel, water infiltrates and fills the pore space of the graben shear banding slope. Therefore, the shear banding graben slope at the north entrance of the Zhongliao Tunnel may also experience slope sliding failure after its completion.

The authors of this paper conducted slope stability analysis using double sliding surfaces composed of shear bands and shear texture planes. The following conclusions are drawn based on the results:

1) When tunnels contain faults or shear bands, and the tunnel structure is intact without fractures at both ends of the fault or shear band, local instability may occur within the fault or shear band. However, this instability typically does not induce overall instability of the tunnel.

2) Upon excavation of a locally unstable fault or shear band into a graben, the slopes on both sides of the graben become significantly unstable,

especially after water infiltration from above into pore spaces in the shear zone.

3) After the shear band tunnel is excavated into a graben, the primary factors influencing graben slope stability are groundwater filling the pore space of the shear band, followed by the softening of shear resistance strength along the sliding surface induced by shear banding.

Based on these conclusions, the authors suggest the following:

1) Although current slope stability regulations do not explicitly stipulate that tunnels must not be excavated into shear bands in grabens, it is recommended that such excavations are not conducted because shear band graben slopes are prone to sliding damage.

2) Given that water sources above tunnels readily infiltrate shear bands and seriously endanger the stability of the shear graben slope, water sources such as mountain lakes above the shear band graben must be removed to reduce the impact of groundwater on slope stability.

References

Google Earth, Website: http://www.google.com.tw/intl/zh-TW/earth/, 2019.

Hsu,Tse-Shan, Wu, Zong-Lin, Lin, Chihsen T., Huang, Yi-Min , "The Major Cause of Anchor Block Slope Failures," International Journal of Organizational Innovation, Vol. 11, No. 2, pp. 175-198, 2018.

Taiwan Geotechnical Society, Formosa highway 3.1K collapse incident investigation report, commissioned by the Ministry of Transportation, 2011.

Taiwan Highway Bureau, Ministry of Transportation and Communications, “The Technical Seminar on Long-term Improvement of National Highway No. 3 Tianliao Viaduct and Zhongliao Tunnel,” Proceedings, 2016.